Purcell-Factor-Enhanced Scattering from Si Nanocrystals in an Optical Microcavity

T. J. Kippenberg,[1,3,4] A. L. Tchebotareva,[2] J. Kalkman,[2] A. Polman,[2,*] and K. J. Vahala[1,†]

[1]*California Institute of Technology, Pasadena, California 91125, USA*

[2]*Center for Nanophotonics, FOM Institute AMOLF, Kruislaan 407, 1098SJ, Amsterdam, The Netherlands*

[3]*Max Planck Institute für Quantenoptik, 85748 Garching, Germany*

[4]*École Polytechnique Fédérale de Lausanne (EPFL), CH-1015 Lausanne, Switzerland*

(Received 17 February 2009; published 10 July 2009)

Scattering processes in an optical microcavity are investigated for the case of silicon nanocrystals embedded in an ultra-high-Q toroid microcavity. Using a novel measurement technique based on the observable mode splitting, we demonstrate that light scattering is highly preferential: more than 99.8% of the photon flux is scattered into the original doubly degenerate cavity modes. The large capture efficiency is shown to result from the Purcell enhancement of the optical density of states over the free space value, an effect that is more typically associated with spontaneous emission. The experimentally determined Purcell factor has a lower bound of 171.

DOI: 10.1103/PhysRevLett.103.027406 PACS numbers: 78.67.Bf, 42.60.Da, 42.65.Yj, 42.81.Qb

Optical microcavities find application in a variety of applied and fundamental studies [1], and in nearly all embodiments subwavelength defect centers are present that lead to scattering. Here we analyze the effect of scattering in an optical microcavity, using a toroid microcavity containing silicon nanocrystals (Si NCs) [2] as scattering centers. Using a novel measurement technique we demonstrate that light scattering is highly preferential; 99.8% of all scattered light is scattered into the original eigenmodes. This value cannot be explained by the existing geometrical optics theory [3]. A theoretical analysis shows that the observed enhanced scattering rate into the original cavity mode is due to the enhancement of the optical density of states over the free space value, and therefore has the same origin as the Purcell effect [4–6] in spontaneous emission. The connection that the local density of states underlies enhanced *scattering* was first noted in Ref. [7]. The result is also consistent with a recent theoretical and experimental analysis of controlled coupling of counterpropagating modes in whispering gallery resonators [8]. Extending the model first introduced in Ref. [8], we show theoretically that the power scattered into the microcavity is enhanced by the Purcell factor and provide a method to extract the Purcell factor experimentally. The presented experimental and theoretical results establish the significance of the Purcell factor for scattering processes within a microcavity and constitute the highest experimentally measured Purcell factor to date (171).

It is a well-known phenomenon [3,9,10] that the resonances of whispering gallery mode (WGM) microcavities [3,9–11] appear as doublets. The doublet splitting is due to lifting of the twofold degeneracy of the clockwise (CW) and counterclockwise (CCW) WGMs that occurs when these modes are coupled due to scattering [3]. In what follows, it is shown how the experimentally observable mode splitting can be directly used to infer the *capture efficiency* (η), defined as the fraction of light scattered into the original eigenmodes, and which, therefore, does not contribute to cavity losses [12].

For a single nanoparticle scattering center, with cross section σ_s and a number density N, the total scattering rate is given by $\gamma_{\mathrm{tot}} = \sigma_s N \frac{c}{n}$, where c is the speed of light. The mode splitting (γ, in the frequency domain) is then given by $\gamma = \frac{1}{2}\eta\gamma_{\mathrm{tot}}$. The factor of $\frac{1}{2}$ takes into account that the scattering of light into original eigenmodes (i.e., self-coupling) does not contribute to the observed mode splitting. Owing to the small size of the scattering centers in comparison to the wavelength of light, it is assumed that scattering is equally divided into CW and CCW direction (i.e., Rayleigh scattering limit). The cavity dissipation rate is given by $\tau^{-1} = (1-\eta)\gamma_{\mathrm{tot}} + \frac{\sigma_a}{\sigma_s}\gamma_{\mathrm{tot}}$, where the term involving σ_a (the absorption cross section of the scattering centers) accounts for absorptive loss associated with the scattering centers. In addition, the rate $1/\tau_0$ is introduced and describes other loss mechanisms not resulting from the scattering centers. The total cavity Q is then given by $Q = \omega(1/\tau_0 + 1/\tau)^{-1}$. The degree to which the scattering process couples the initially degenerate cavity modes can be described by the modal coupling parameter Γ [10]:

$$\Gamma = \left(\frac{\frac{1}{2}\eta\gamma_{\mathrm{tot}}}{\tau_0^{-1} + (1-\eta)\gamma_{\mathrm{tot}} + \frac{\sigma_a}{\sigma_s}\gamma_{\mathrm{tot}}}\right). \tag{1}$$

Thus, Γ reflects the relative "visibility" of the doublet as appearing in the undercoupled resonance spectrum [9,10].

The capture efficiency η can be retrieved from Γ as follows. In the presence of other loss channels, such as residual material absorption, two limits of Eq. (1) can be considered. First, if the cavity losses are dominated by non-scattering-center related loss, i.e., the absorption-limited case $\tau_0^{-1} \gg (1-\eta)\gamma_{\mathrm{tot}} + \frac{\sigma_a}{\sigma_s}\gamma_{\mathrm{tot}}$, Eq. (1) simplifies to

$$\lim_{\tau_o^{-1} \gg \gamma_{\mathrm{tot}}} \Gamma = \frac{1}{2}\eta\gamma_{\mathrm{tot}}\tau_0 = \frac{\eta\gamma_{\mathrm{tot}}}{2\omega}Q_0; \tag{2}$$

i.e., Γ measured for different cavity modes increases linearly with intrinsic $Q_0 \equiv \omega\tau_0$ (if it is assumed that scattering is constant for all cavity modes). In this regime, a *lower bound* of the capture efficiency η can be found, given by $\eta > 2\omega\Gamma/Q_0\gamma_{\mathrm{tot}}$.

Second, in the scattering-center-limited case, and assuming τ_o is constant (i.e., non-scattering-center absorption is fixed), it is useful to rewrite Eq. (1) in terms of total Q where $Q_{\mathrm{tot}}^{-1} \equiv Q_0^{-1} + Q_{\mathrm{scat}}^{-1}$ with $Q_{\mathrm{scat}} \equiv \omega\tau$,

$$\Gamma = \frac{1}{2}\frac{\eta}{1-\eta+\frac{\sigma_a}{\sigma_s}}\left[1-\frac{Q_{\mathrm{tot}}}{\omega\tau_0}\right]. \tag{3}$$

This equation shows that a signature of this regime will be a *decreasing* linear dependence of Γ on total Q. Furthermore, in such a Γ vs Q_{tot} plot, the Q-axis intercept (Q_x) gives the non-scattering-center loss through $\omega\tau_o = Q_x$, while the Γ intercept (Γ_x) yields the following relation: $\eta = \frac{2\Gamma_x}{1+2\Gamma_x}(1+\frac{\sigma_a}{\sigma_s})$. Significantly, this shows that measurement of Γ_x provides another important lower bound on capture efficiency through the relation $\eta > 2\Gamma_x/(1+2\Gamma_x)$. Moreover, the functional differences in the dependence of Γ vs Q determine whether the cavity is operating in the *absorption* or *scattering* loss dominated regime. To test the above model, we have investigated the scattering processes of SiO_2 toroid microcavities [13,14].

Figure 1 shows measurements of the Γ parameter for an undoped SiO_2 50-μm-diameter toroid microcavity, measured for successive fundamental resonances with different Q in the 1550 nm band. A cavity resonance scan is provided in the upper-right-hand panel of Fig. 1, and shows the typical doublet splitting of ~10 MHz observed for pure SiO_2 toroids. The data in the main panel of Fig. 1 clearly follow a positive-slope, linear relationship, indicating that the cavity resonances follow absorption-limited behavior

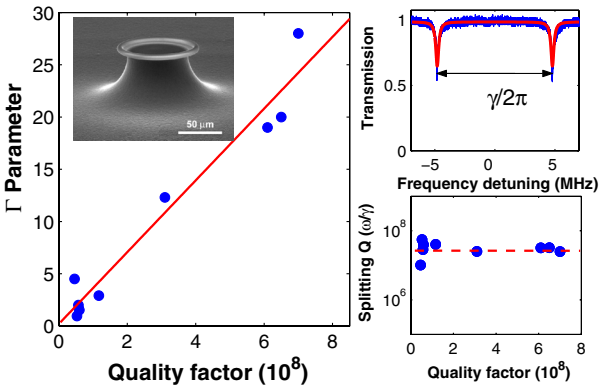

FIG. 1 (color online). Left: Modal coupling parameter (or doublet "visibility") Γ as a function of Q for several fundamental modes of a SiO_2 toroid microcavity. A scanning electron micrograph of a toroid microcavity is shown as the inset. Upper right-hand panel: Characteristic spectral scan, showing a typical mode splitting of ~10 MHz and $\Gamma \sim 30$. Lower right-hand panel: Splitting Q_{split} ($=\omega/\gamma$) as a function of Q, which is nearly identical for all modes of the resonator.

(attributed to adsorbed water and OH on the surface of the toroid [15]). The scattering rate $\gamma/2\pi$ derived from the data is plotted in the lower-right-hand figure, and is indeed, to a very good approximation, the same for all modes. From the highest observed doublet splitting ($\Gamma = 28$) the lower estimate of the capture efficiency is $\eta > 96.4\%$. This value cannot be explained by the quasigeometrical estimations of Ref. [3] which predict a *maximum* capture efficiency of 90%. This model assumes that scattered light obeys a Rayleigh-type angular distribution, and can couple back into the CW and CCW modes, provided the scattering angle θ is within the critical angle ϕ of the mode. This model, while adequate to describe losses of a waveguide bend, is (as shown below) incomplete as it neglects enhancement of the scattering through the Purcell effect.

To infer η more exactly, measurements were performed in the scattering-center-limited regime, by fabricating SiO_2 toroid microcavities doped with Si NCs. Si NCs exhibit quantum-confined photoluminescence (PL) in the visible and near infrared. Si NCs do not possess significant absorption transitions at $\lambda = 1.5$ μm and have a high refractive index relative to the SiO_2 matrix ($n = 3.48$ vs $n = 1.44$) and thus act (in the 1550-nm band) as strong scattering centers. The Si NC doped cavities were made by ion implantation of 900 keV Si^+ ions (fluence 9.1×10^{16} cm^{-2}) into a thermally oxidized Si wafer (2 μm oxide), followed by annealing and toroid fabrication. In order to confirm the presence of Si NCs after fabrication, 2D cross-sectional PL images were measured. A bright luminescent ring is observed, characteristic of emission from Si NCs. The emission spectrum (cf. Fig. 2) peaks at $\lambda = 675$ nm, corresponding to a NC diameter of ~3 nm.

The optical resonances of Si NC doped microcavities exhibited splitting frequencies as large as 1 GHz. The highest observed modal coupling parameter was $\Gamma = 50$. Despite strong scattering from the NCs, a $Q > 10^7$ is attained for most resonances.

Two different sets of transverse cavity modes (attributed to the radial mode index $n = 1$ and $n = 2$) were characterized with progressing angular mode numbers ($\ell, \ell+1, \ell+2, \ldots$). Because of the inhomogeneous distribution of the NCs (cf. Fig. 2), these modes are dominated by differing levels of scattering. However, due to the presence of water and OH adsorbed onto the cavity surface, each set of radial modes experiences the same amount of residual absorption. Γ vs Q_{tot} measurements for each of these resonances are shown in Fig. 3. Two clear, linear behaviors are present, representative of absorptive and scattering-center-limited regimes. The solid line (negative slope) in Fig. 3 is attributed to the $n = 1$ radial modes and is scattering-center limited. From the observed behavior, the quantity Γ_x was determined. Using Eq. (3), we obtain $\eta > 99.42\%$ ($\pm 0.04\%$) and $\tau_0 = 115$ ns (± 3 ns) (i.e., $Q_0 = 1.4 \times 10^8$). The positive slope data (absorptive limited regime) are attributed to the $n = 2$ radial modes, which possess increased intrinsic (OH and water) absorption losses, owing to their slower decaying field amplitude

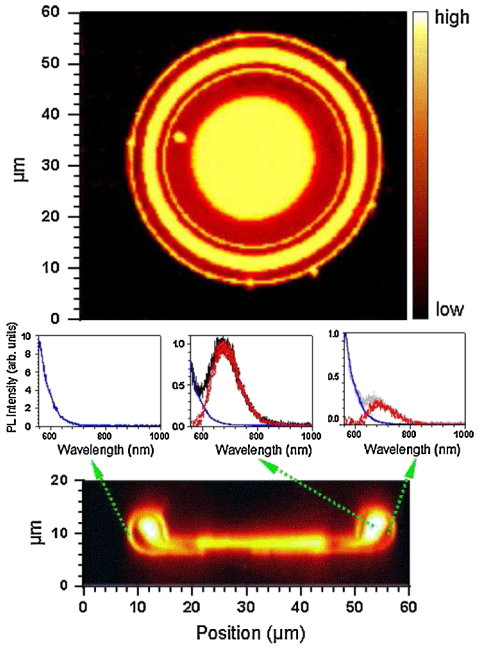

FIG. 2 (color online). Cross-sectional confocal PL images taken on a 72-μm-diameter Si NC doped SiO_2 toroidal microcavity. Photoluminescence is collected in 650–690 nm band. (a) x-y cross section. (b) y-z cross section. Both images are taken with the toroid immersed into index-matching oil doped with rhodamine. The insets show PL spectra taken at characteristic locations in the toroid. The outer bright line in both images is attributed to the PL of the rhodamine dye and serves to determine the cavity's outer contour.

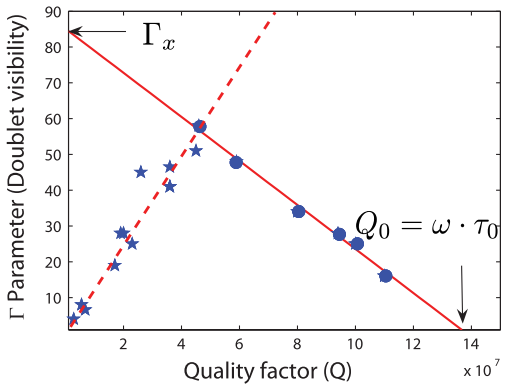

FIG. 3 (color online). Normalized splitting parameter (Γ) as a function of Q for the microcavity from Fig. 2. The solid line is a linear fit to Eq. (3) in the scattering-limited regime (closed circles), yielding $\tau_0 = 115.2 \pm 3$ ns, and $\eta = 99.42 \pm 0.04\%$. The low Q data (stars), fitted with the dashed line, correspond to higher-order (absorption-limited) radial modes [Eq. (2)]. The extrapolated intercept of the data with the vertical axis yields a lower bound for the scattering efficiency (Γ_x).

outside the cavity. This mode identification is also consistent with the inhomogeneous distribution of NCs, which causes increased scattering for higher-order radial modes (cf. Fig. 2). The inferred intrinsic cavity lifetime τ_0 is in good quantitative agreement with estimates of the absorption loss due to water adsorbed onto the cavity surface [15]. The remarkably high lower bound on capture efficiency of 99.42% found here clearly demonstrates that optical scattering in microcavities occurs highly preferentially into cavity eigenmodes.

The role of the Purcell effect in the scattering process was first noted in Ref. [7], and was later analyzed in the role of coupling CW and CCW modes via an evanescent scattering center [8]. However, the precise way in which the Purcell factor enters has so far not been described. Here, extending the model of Ref. [8], we show that the scattering between CW and CCW mode is precisely enhanced by the Purcell factor. Central to Purcell's original analysis [4] is the use of both quasimodes and continuum modes to explain enhanced spontaneous emission from a dipole emitter within a cavity. Along these lines, the local density of continuum modes is higher within the cavity (by the Purcell factor) and the spontaneous decay rate for an atom in resonance with a cavity mode is enhanced by the same factor (via Fermi's golden rule). This overall rate enhancement is proportional to Q/V, where Q is the cavity's optical Q factor and V is the mode volume. Extending the model introduced previously in Refs. [3,8], scattering of a resonator mode by a point defect into a continuum mode is described by

$$\dot{a}_{\mathbf{k}} = -\imath\omega_{\mathbf{k}} a_{\mathbf{k}} - \imath\alpha\sqrt{\frac{\omega_o \omega_{\mathbf{k}}}{4V_{\mathrm{CW}} V_{\mathbf{k}}}}\, a_{\mathrm{CW}}, \tag{4}$$

where $a_{\mathbf{k}}$ (a_{CW}) is the lowering operator for a continuum (resonator) mode with wave vector $\mathbf{k}$ (index CW) and frequency $\omega_{\mathbf{k}}$. The index CW in this case signifies a clockwise mode of a whispering gallery resonator, α is the polarizability of the scattering center, and, for reasons that will become apparent, the polarization of all modes is taken to be the same. The scatterer is assumed to be at a maximum of the cavity's spatial mode, and, for the initial portion of this analysis, the continuum modes are treated as discrete by use of a large quantization volume (V_k). This equation is now used to investigate the role of the Purcell effect in backscatter coupling.

The electric field amplitude for the CCW resonator mode can be constructed by summation over only those continuum modes that comprise the CCW mode, i.e., $\sqrt{\frac{\omega_o}{2V_{\mathrm{CCW}}}}\, a_{\mathrm{CCW}} = \sum_{\mathbf{k}_{\mathrm{CCW}}} \sqrt{\frac{\omega_{\mathbf{k}}}{2V_{\mathbf{k}}}}\, a_{\mathbf{k}}$ followed by substitution using the integral form of Eq. (4). The notation $\mathbf{k}_{\mathrm{CCW}}$ indicates the above restriction on the summation over $\mathbf{k}$. Because the mode volume is different for continuum (V_k) and resonator modes ($V_{\mathrm{CCW,CW}}$), it is essential that this summation be performed with respect to electric field amplitudes (as opposed to lowering operator amplitudes). In analogy to the standard Weisskopf-Wigner [16] treatment of spontaneous emission, the quantization volume is subsequently enlarged so that the summation becomes an integration over the continuum making up the CCW mode.

$$\sqrt{\frac{\omega_o}{2V_{\mathrm{CCW}}}}a_{\mathrm{CCW}} = -\imath\alpha\sqrt{\frac{\omega_o}{2V_{\mathrm{CW}}}}\int_{-\infty}^{t} d\tau a_{\mathrm{CW}}(\tau) \times \int_{\mathbf{k}_{\mathrm{CCW}}} \frac{d\mathbf{k}}{(2\pi)^3}\frac{\omega_{\mathbf{k}}}{2}e^{-\imath\omega_{\mathbf{k}}(t-\tau)}. \quad (5)$$

Since all quantities within the integral over $\mathbf{k}$ depend upon $\omega_{\mathbf{k}}$, a density of modes function is introduced to enable integration over frequency, via $\int_{\mathbf{k}_{\mathrm{CCW}}} \frac{d\mathbf{k}}{(2\pi)^3} \rightarrow \frac{1}{V_{\mathrm{CCW}}}\int d\omega \frac{\kappa/2\pi}{(\omega-\omega_o)^2+(\kappa/2)^2}$. This density function is precisely the *Purcell density of states* since it characterizes the dipole scattering into modes that comprise the CCW mode of the resonator, where ω_o and $\kappa = \tau^{-1} + \tau_0^{-1}$ are the frequency and the decay rate of the CCW (and CW) resonator mode. In writing this expression, the mode density has been expressed as a Lorentzian, normalized so that, upon integration, there is precisely one mode per cavity linewidth. The integration with respect to frequency is now performed yielding the result $a_{\mathrm{CCW}}(t) = -\imath\alpha\frac{\omega_o}{2V} \times \int_{-\infty}^{t} d\tau a_{\mathrm{CW}}(\tau)e^{-\imath\omega_o(t-\tau)}e^{-(\kappa/2)(t-\tau)}$, where $V_{\mathrm{CCW}} = V_{\mathrm{CW}} \equiv V$ has been used. For a scattering center that is driven at a frequency resonant with the cavity, this integral equation enables construction of the following power coupling equation between the CW and CCW modes,

$$\dot{p}_{\mathrm{CCW}} = -\kappa p_{\mathrm{CCW}} + \alpha^2\frac{\omega_o Q}{V^2}p_{\mathrm{CW}}, \quad (6)$$

where p_{CCW} is the power in the CCW mode ($p_{\mathrm{CCW}} \propto a_{\mathrm{CCW}}a^*_{\mathrm{CCW}}$) and p_{CW} is the drive power at frequency ω_o in the clockwise mode. The coefficient of p_{CW} gives the scattering rate of CW into CCW optical power caused by scattering from the point defect. The defect will also produce Rayleigh scattering into the other (i.e., noncavity continuum modes). When this isotropic scattering rate [$\Gamma_{\mathrm{iso}} = \alpha^2\omega_0^4/(6\pi c^3 V)$] [8] is used to normalize the CW to CCW coupling, a remarkable result is apparent:

$$\frac{1}{\Gamma_{\mathrm{iso}}}\alpha^2\frac{\omega_o Q}{V^2} = \frac{3}{4\pi^2}\lambda^3\frac{Q}{V}. \quad (7)$$

The final expression here is none other than the Purcell factor [4,5], well known in the context of spontaneous emission enhancement in cavity QED [4–6]. This result essentially states that the observed enhancement of collection efficiency is entirely the result of the local density of mode enhancement caused by the Purcell effect. The result also establishes a precise relationship between the collection efficiency and the Purcell factor expressed as follows:

$$F = \frac{\eta}{1-\eta}. \quad (8)$$

Using this expression and the lower bound on η of 99.42% yields a measured Purcell factor of at least 171.

This is the highest Purcell factor measured to date. Theoretically, the Purcell factor for the toroid microcavities used in the experiments ($Q = 1.3 \times 10^8$, $D = 72\ \mu$m, $A_{\mathrm{eff}} = 14\ \mu\mathrm{m}^2$) equals $F = 2060$, corresponding to $\eta = 99.95\%$. The discrepancy between this and the experimentally found value is likely to be caused by the presence of minute absorption. Finally, it is noted that the largest observable mode splitting (i.e., Purcell factor) is necessarily bound by the fact that the scattering center itself limits the cavity Q (and correspondingly the Purcell factor). Indeed, in this scattering dominated regime, the largest ratio of mode splitting is given by the expression $\Gamma_{\mathrm{max}} = 3\lambda^3/4\pi^2\alpha = 3\lambda^3/(16\pi^3 a^3)\frac{n^2+2}{n^2-1}$ [8] for a spherical scattering particle of radius a and refractive index n. Analysis reveals that for silicon nanocrystals of size 3 nm this would—in the absence of absorption mechanisms—allow observation of a Purcell factor exceeding 10 000 for the cavity used in this work.

We thank Professor S. Roorda for ion implantation. This work was funded by the DARPA and the Alexander von Humboldt Foundation. The Dutch part of this work is part of the research program of FOM. T. J. K. acknowlegdes support by the Nanosystems Initiatitve Munich (NIM) and the Max Planck Society.

*polman@amolf.nl
†vahala@caltech.edu

[1] K. J. Vahala, Nature (London) **424**, 839 (2003).
[2] M. L. Brongersma, P. G. Kik, A. Polman, K. S. Min, and H. A. Atwater, Appl. Phys. Lett. **76**, 351 (2000).
[3] M. L. Gorodetsky, A. D. Pryamikov, and V. S. Ilchenko, J. Opt. Soc. Am. B **17**, 1051 (2000).
[4] E. M. Purcell, Phys. Rev. **69**, 37 (1946).
[5] P. Milonni, *The Quantum Vacuum* (Academic, New York, 1994).
[6] S. Haroche and D. Kleppner, Phys. Today **42**, No. 1, 24 (1989).
[7] T. J. Kippenberg, A. L. Tchebotareva, J. Kalkman, A. Polman, and K. J. Vahala, in *Proceedings of the Quantum Electronics and Laser Science Conference (QELS), Baltimore, MD, 2005* (Optical Society of America, Washington, DC 2005), pp. 62–64.
[8] A. Mazzei, S. Götzinger, L. Menezes, G. Zumofen, O. Benson, and V. Sandoghdar, Phys. Rev. Lett. **99**, 173603 (2007).
[9] D. S. Weiss, V. Sandoghdar, J. Hare, V. Lefevreseguin, J. M. Raimond, and S. Haroche, Opt. Lett. **20**, 1835 (1995).
[10] T. J. Kippenberg, S. M. Spillane, and K. J. Vahala, Opt. Lett. **27**, 1669 (2002).
[11] M. Borselli, K. Srinivasan, P. Barclay, and O. Painter, Appl. Phys. Lett. **85**, 3693 (2004).
[12] The definition of η is thus analogous to that of the spontaneous emission coupling factor.
[13] D. K. Armani, T. J. Kippenberg, S. M. Spillane, and K. J. Vahala, Nature (London) **421**, 925 (2003).
[14] S. M. Spillane, T. J. Kippenberg, O. J. Painter, and K. J. Vahala, Phys. Rev. Lett. **91**, 043902 (2003).
[15] H. Rokhsari and K. J. Vahala, Appl. Phys. Lett. **85**, 3029 (2004).
[16] M. O. Scully and M. S. Zubairy, *Quantum Optics* (Cambridge University Press, Cambridge, England, 1996).